


PAPER

Cite this: *Nanoscale*, 2019, **11**, 1228

Moisture-tolerant supermolecule for the stability enhancement of organic–inorganic perovskite solar cells in ambient air†

Dong Wei,^a Hao Huang,^a Peng Cui,^a Jun Ji,^a Shangyi Dou,^a Endong Jia,^b Sajid Sajid,^a Mengqi Cui,^a Lihua Chu,^a Yingfeng Li,^a Bing Jiang^a and Meicheng Li *^a

Instability of the perovskite materials, especially in high humidity, is one of the major limitations that hinders the development of perovskite devices. Herein, to eliminate the degradation of perovskite solar cells in humid air, a water-resistant perovskite absorption layer is proposed by introducing a macrocycle-type cyclodextrin material (β -CD) into the films. The β -CD was proved to be capable of facilitating the crystallization of grains and enhancing the stability of the perovskite by forming supramolecular interactions with organic cations through the hydrogen bonding in the perovskite films. Consequently, the average efficiency of the PSCs remarkably increased from 16.19% to 19.98%. The champion solar cell even delivered an efficiency of 20.09%. The PSCs with β -CD exhibited superior long-term stability in ambient air without encapsulation, which retained 90% of the initial efficiency after continuous AM 1.5 illumination in ambient air with 80% humidity for 300 h.

Received 19th September 2018,

Accepted 9th December 2018

DOI: 10.1039/c8nr07638c

rsc.li/nanoscale

Introduction

Organic–inorganic hybrid perovskite materials (OIPs) have received extraordinary attention due to their excellent properties, such as long carrier diffusion lengths, low recombination rates and a strong optical absorption. They are considered to be the most promising active materials for the applications in photovoltaic devices due to their outstanding optoelectronic properties.^{1–7} The rapid development of perovskite solar cells (PSCs) in recent years from 3.8% in 2009 to 23.3% in 2018, is associated with the important studies that provided important insights into the precursor chemistry of the perovskite coating and reported the long-term stable solid-state perovskite solar cells.^{8–13} Even with these remarkable achievements, the issue of instability of PSCs, especially under humid conditions, remains unresolved. The hydrated intermediate structures (such as $\text{MAPbI}_3 \cdot \text{H}_2\text{O}$ and $\text{MA}_4\text{PbI}_6 \cdot 2\text{H}_2\text{O}$) tend to form strong interactions between water molecules and perovskite materials, leading to the total irreversible degradation of OIPs

to lead iodide.^{14–17} Hence, it is crucial to improve the stability of OIPs for enhanced performance and stability of PSCs in high humidity.

To improve the stability of OIPs under humid conditions, a number of attempts have been made. One strategy is to introduce a protective layer over the perovskite to block the corrosion of perovskite materials by moisture. Many functional materials, such as fluoro-silane,¹⁸ silane-functionalized fullerene,¹⁹ and CuSCN ²⁰ have been fabricated as water-resistant layers, which have been demonstrated to be efficient in inhibiting the degradation of perovskite materials in ambient environment. Another strategy is to enhance the stability of perovskite films by integrating cross-linkable materials into perovskite films. This can prevent the perovskite from interacting with water by straining the organic compound and the inorganic compound of the perovskite through hydrogen bonding.^{21,22} Based on this strategy, various types of cross-linkable materials, such as polyethylene glycol and 2-aminoethanethiol, have been blended into perovskites. As a result, the improved stability of perovskite films and even the promotion of nucleation and growth of perovskite grains were achieved.²³ Therefore, doping additives into perovskite materials for enhancing the stability of perovskite films has been well proved to be an effective approach to eliminate the degradation of PSCs in a humid atmosphere. However, most of these efforts just focus on enhancing the stability of perovskite films or PSCs under humid conditions, rather than under working conditions in high-humidity air. Hence, it is impor-

^aState Key Laboratory of Alternate Electrical Power System with Renewable Energy Sources, School of Renewable Energy, North China Electric Power University, Beijing 102206, China. E-mail: mcli@ncepu.edu.cn; Fax: +86 10 6177 2951; Tel: +86 10 6177 2951

^bKey Laboratory of Solar Thermal Energy and Photovoltaic System, Institute of Electrical Engineering, Chinese Academy of Sciences, Beijing 100190, China

†Electronic supplementary information (ESI) available. See DOI: 10.1039/c8nr07638c

tant to find out a kind of neutral molecule that could improve the stability of perovskite materials and devices under practical working conditions. These enhanced PSCs with long-term stability and high efficiency possess prospects for commercial applications in the future.

Herein, through thoughtful analysis and design, we utilized the β -cyclodextrin (β -CD) macrocycle as a stability-enhancing additive doped into the perovskite precursor to form a stable perovskite absorptive layer and explored the beneficial effect of introducing it into planar PSCs. The doped β -CD improved both the humidity stability and the illumination stability of the perovskite. Moreover, the doped β -CD promoted the nucleation and growth of perovskite grains to obtain more compact and smoother perovskite films, which is the core of high performance PSCs. Consequently, the PCE of the planar PSCs with β -CD exhibited a significant increase from 17.17% to 20.09%, compared to that of standard planar PSCs. After a continuous illumination in ambient air for 300 h, the PSCs with β -CD retained about 90% of the initial efficiency. This macrocycle-type cyclodextrin material is one representative

choice among legions of hydroxyl-rich molecules for demonstrating the viability of the doping process with functional materials in perovskite films, highlighting its promise for improving the performance and stability of PSCs.

Results and discussion

The molecular structure of β -cyclodextrin (β -CD) and the schematic illustration of the interactions between β -CD and the perovskite are shown in Fig. 1a and b. As shown in Fig. 1a, the molecule of β -CD is a glucose-based cyclic oligosaccharide, which consists of seven glucopyranose units and forms a torus-shaped ring structure. These glucopyranose units possessing many hydroxyl groups at the external CD surfaces may introduce strong interactions with CH_3NH_3^+ (MA^+) ions in the perovskite lattice.²⁴ To clarify the interaction between MA^+ cations and β -CD, the interaction energies were computed by density functional theory (DFT) (WASP 5.0 software). The hydrogen-bonding interaction between MA^+ cations and β -CD

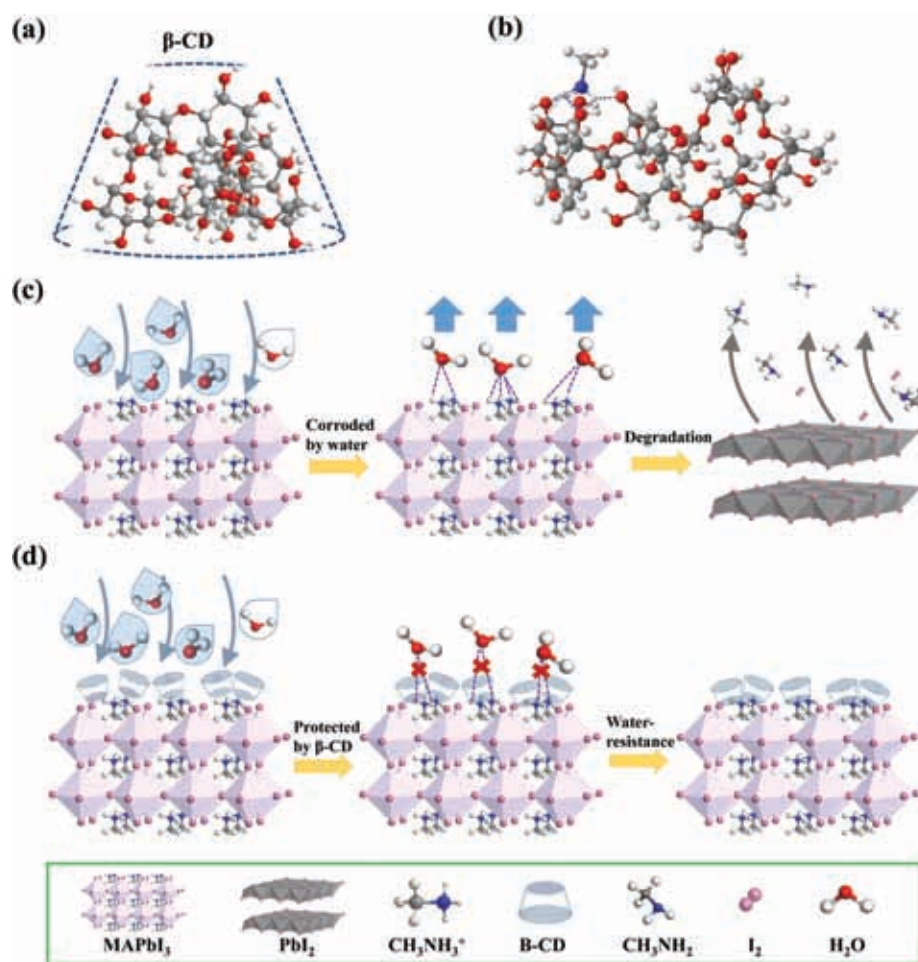


Fig. 1 (a) Molecular structure of β -cyclodextrin; (b) schematic diagram to show the interactions between the perovskite and β -cyclodextrin molecules; schematic diagram to show the mechanisms for (c) the degradation process of the pristine perovskite and (d) the water-resistant property of the perovskite with β -CD.

is demonstrated in view of an optimized geometry with the largest interaction energy, as shown in Fig. 1b. The interaction energy of MA^+ - β -CD was calculated to be $-46.75 \text{ kcal mol}^{-1}$, which is nearly three times higher than the interaction energy between MA^+ and H_2O ($-14.61 \text{ kcal mol}^{-1}$). Thus, β -CD could firmly anchor the MA^+ cations and then prevent them from interacting with H_2O in ambient air. Moreover, the hydrogen bonds of the β -CD molecule are able to interact with I^- ions on the frame of the perovskite, which induce a stronger interaction between organic cations and halide ions in the perovskite lattice.^{25,26} Hence, it could be expected that the framework of the fabricated perovskite films would be enhanced drastically owing to the strong interaction between β -CD and the perovskite, which is very critical for obtaining more stable perovskite films and devices. According to Fig. 1d, the doped β -CD secures the MA^+ and protects these organic cations from water erosion, which enables the perovskite materials to possess more stable properties in moisture conditions compared to the pristine perovskite, as shown in Fig. 1c. On account of the benefits of β -CD, we blended various amounts of β -CD molecules into the MAPbI_3 -based perovskite precursor to construct stable PSCs with the n-i-p structure: ITO/ SnO_2 /perovskite (with or without β -CD)/spiro-OMeTAD/Au, as shown in ESI Fig. S1.†

To understand the effects of β -CD on the morphology of perovskite films, scanning electron microscopy (SEM) has been performed on the fresh perovskite films without and with β -CD, as shown in Fig. 2a and b, respectively. In Fig. 2a, the pristine perovskite film is compact and smooth, and the average size of the perovskite grains is about 300 nm. In comparison, the perovskite film with β -CD evidently presents more

compact grains and bigger grain size in Fig. 2b, which indicates better crystallization. The average-diameter statistics of the perovskite films with and without β -CD are also exhibited in Fig. S2.† From Fig. S2,† it is clear that the counts of large-sized grains (larger than 500 nm) constitute about 80% of the total circled grains in the perovskite film with β -CD, which demonstrates that the perovskite film with β -CD has more large-sized and well-crystallized grains than the perovskite film without β -CD. Moreover, the morphologic images of the long-term operated perovskite films without and with β -CD are also exhibited in Fig. 2c and d, respectively. The operating conditions were under AM 1.5 illumination at 90°C in ambient air with a humidity of 80% for one week, as shown in Fig. S3.†

The morphology of the perovskite film without β -CD after a long-term operating process had changed entirely as seen in Fig. 2c. The perovskite film possessed a cavity-textured rough surface, in which these perovskite grains suffered from serious water corrosion and damage in air. This indicates that the pristine perovskite film is not able to resist the violent destruction from water and illumination as reported elsewhere.^{27–30} On the contrary, the surface image of the perovskite film with β -CD after the operation process changed only a little compared to that of the fresh perovskite film. In Fig. 2d, the morphology of the analyzed film demonstrates small-sized grains without any pin-holes compared to Fig. 2c, which indicates that the doped β -CD delays the degradation of the perovskite significantly. These results accorded very well with the calculation results from DFT. In order to directly exhibit the changes of these perovskite films before and after a long-term operation, the digital photos of these films are also presented in ESI Fig. S4.† It could be observed that the perovskite films

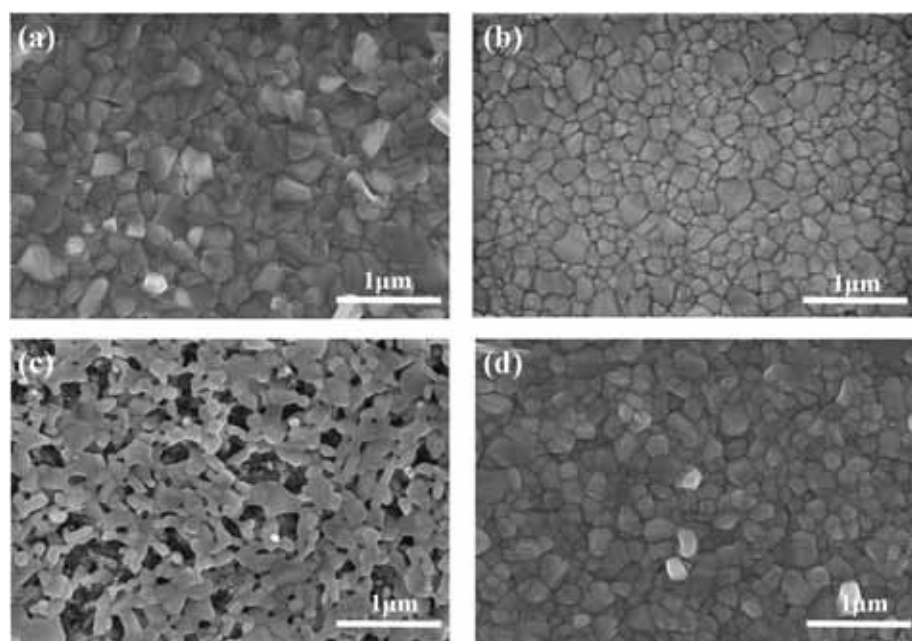


Fig. 2 Surface SEM images of the perovskite films without and with β -cyclodextrin (a, b) before and (c, d) after the operating process. All the films were fabricated on SnO_2 substrates.

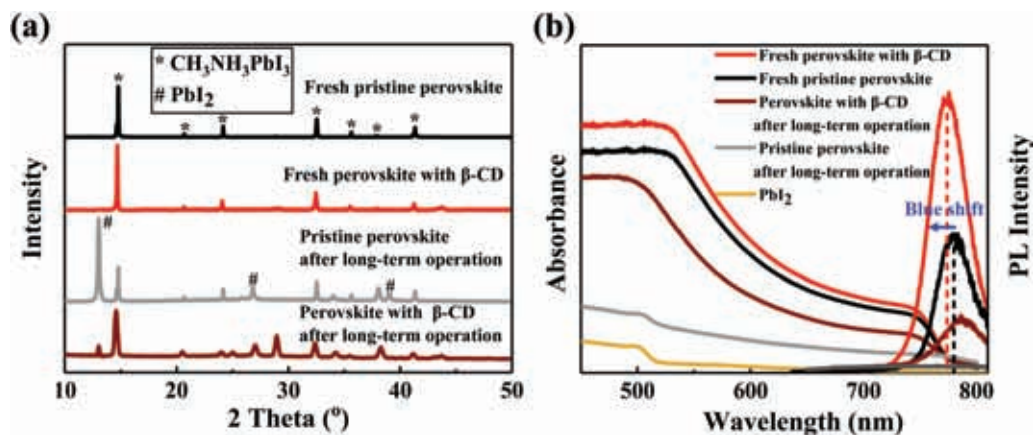


Fig. 3 (a) XRD patterns of the perovskite films without and with β -cyclodextrin, before and after the long-term operating process; (b) absorption and PL spectra of the perovskite films without β -cyclodextrin and with β -cyclodextrin, before and after the long-term operating process.

without β -CD became yellow after a long-term operation, which was considered as the color of PbI_2 . This was confirmed from the above-mentioned SEM results.

The crystalline properties of the perovskite films without and with β -CD were also explored by X-ray diffraction (XRD) measurements. As shown in Fig. 3a, the XRD peaks of the fresh perovskite films without and with β -CD are indexed to the typical diffraction peaks of a perovskite.^{31,32} After a long-term operation, the perovskite film without β -CD exhibited a more intense diffraction peak of PbI_2 located at 12.6° compared to the perovskite film with β -CD, further demonstrating the stronger tolerance of the perovskite film with β -CD to moisture and illumination.^{33,34} In addition, the changes in the optical properties of the as-prepared perovskite films before and after the operating process had also been investigated by UV-Vis absorption, steady-state and time-resolved photoluminescence (PL and TRPL) measurements, as shown in Fig. 3b and Fig. S5.† The structure of the samples for PL and TRPL measurements was a glass/perovskite film. Compared to the pristine film, the perovskite film with β -CD exhibited a stronger absorption in the visible range, which was assigned to the enhanced crystallization and reduced reflection.^{35,36} In Fig. 3b, we can observe that the cut-off edges of the perovskite with β -CD show a slight red shift compared to those of the pristine film. This may be associated with the shrinkage of the optical band gap of perovskite films with β -CD, resulting from the increased grain size.^{37,38} These results coincide exactly with the SEM observations and the XRD analysis. The PL emission peak of the perovskite film with β -CD showed an increased intensity and significant blue shift, indicating the lower number of defects and the higher crystallization of the measured perovskite film.^{39,40} Furthermore, time-resolved photoluminescence (TRPL) spectroscopy was also employed to detect the carrier lifetimes of perovskite films with and without β -CD, as shown in Fig. S5.† The as-measured films were fabricated directly on glasses and excited from the perovskite side with an excitation of 470 nm. All the PL decay curves were monitored at the peak emission of 780 nm and they

could be fitted with two-component exponential decays as in the previous reports.^{41,42} From Fig. S5,† it is evident that the PL decay curve of the perovskite film with β -CD exhibits a longer PL lifetime compared to that of the pristine perovskite film, indicating that the perovskite film with β -CD possesses less defects in bulk.^{43,44} This result is also consistent with the PL result. For the films that were operated for a long time, the absorption and PL spectra of the pristine film changed significantly. The absorption edge of PbI_2 appeared in the spectrum of the pristine film and the PL intensity completely decreased. For the perovskite with β -CD, the spectra of absorption and PL also changed significantly, which confirmed the degradation of perovskite films. However, the damages from the moisture of the films with β -CD were illustrated to be less aggressive compared to those of the pristine films. This is mainly owing to the protection of moisture-sensitive organic cations by β -CD.

To check the influence of the doped β -CD on the performance and the stability of PSCs, MAPbI₃-based perovskite solar cells with various concentrations of β -CD in the perovskite precursor had been prepared and the corresponding current density–voltage (J - V) curves are shown in ESI Fig. S6.† We have collected the short-circuit current density (J_{SC}), open-circuit voltage (V_{OC}), fill factor (FF) and the photoelectric conversion efficiency (PCE) from twenty corresponding PSCs. The average results of these photovoltaic parameters are summarized in Table S1.† It is evident that a significant improvement in device performance is seen in the PSC with a β -CD concentration of 5 mg mL⁻¹ in the perovskite precursor, demonstrating a PCE of 19.98% (16.19% higher than that of the standard planar PSC). The J - V hysteresis of PSCs with and without β -CD was also detected as shown in Fig. S7.† We first measured these devices from V_{OC} to J_{SC} (reverse scan) and then, they were measured from J_{SC} to V_{OC} (forward scan) under AM 1.5G illumination, with a scan rate of 100 mV s⁻¹. It demonstrated that the additional β -CD has a little effect on the improvement of J - V hysteresis. Fig. 4a compares the performances of the champion MAPbI₃-based PSCs with and without β -CD. It can

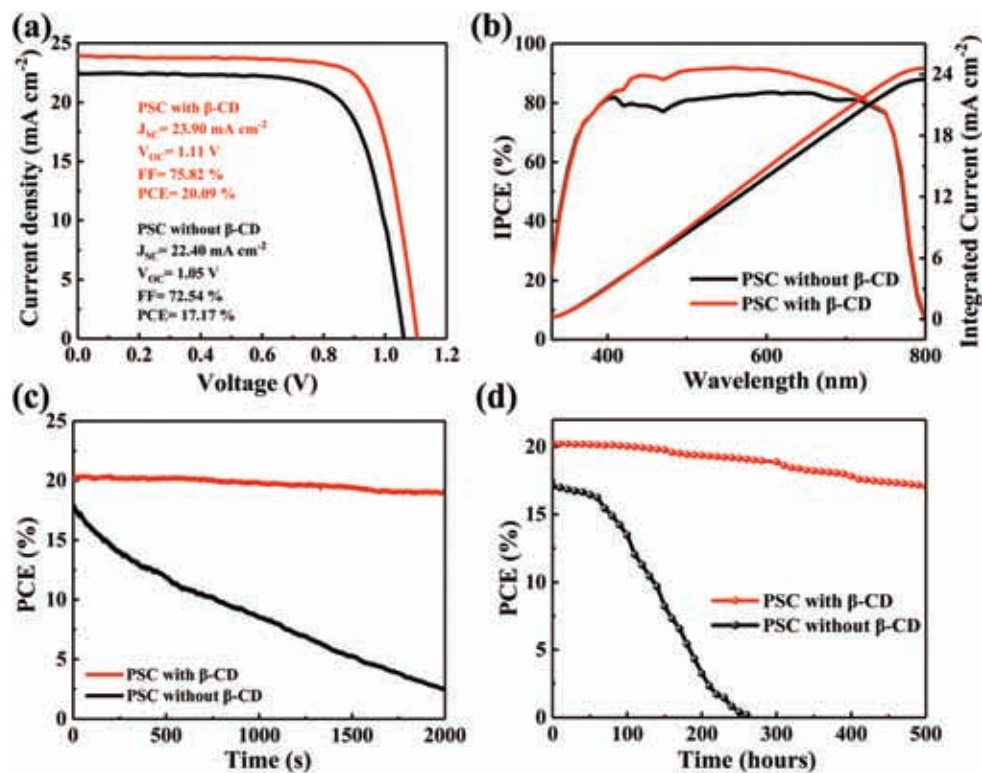


Fig. 4 (a) J - V curves of the champion PSCs without and with β -CD; (b) IPCE curves and the corresponding integrated currents of PSCs without and with β -CD; (c) changes of PCE vs. illumination time of PSCs without and with β -CD, obtained by tracking the maximum power point at 0.95 V; (d) long-term stability of PSCs without and with β -CD for 500 hours.

be seen that the PSCs with β -CD exhibit better performance than the pristine perovskite-based PSCs. The PCE of PSCs increased drastically from 17.17% (the pristine perovskite-based PSC) to 20.09% (perovskite/ β -CD-based PSC). Notably, the improvement of J_{SC} was the largest from 22.40 mA cm^{-2} to 23.90 mA cm^{-2} , among the performance parameters of the devices. To illuminate the improvement of J_{SC} of the PSCs with β -CD, external quantum efficiencies (EQE) of PSCs with and without β -CD were investigated. As shown in Fig. 4b, the PSC with β -CD presents a higher EQE compared to the standard PSC in the wavelength range of 400 nm to 760 nm. The integrated J_{SC} of the PSCs with and without β -CD from the EQE spectra are 24.13 mA cm^{-2} and 22.51 mA cm^{-2} , respectively. The deviations between the integrated J_{SC} and the measured J_{SC} of these PSCs are about 0.4%–0.5%, which illustrates the good consistency between the integrated J_{SC} and the measured J_{SC} . Furthermore, the carrier dynamic characteristics of the two-type perovskite films with the structure of ITO/SnO₂/perovskite had also been investigated by TRPL spectroscopy. As shown in Fig. S8,[†] the PL decay curves present similar profiles for the perovskites with and without β -CD, which illustrates that β -CD has little influence on the carrier transport between perovskite films and electron transport layers. Hence, it can be deduced that the significant increase of J_{SC} in the PSC with β -CD is mainly owing to the reduction of defects in the films, which is confirmed from the PL and XRD results.

For PSCs, the operational stability in ambient air is another critical evaluation. Herein, the aging performance of PSCs with and without β -CD are exhibited in Fig. 4c, by tracking the maximum power point of 0.95 V at room temperature (≈ 25 °C) in ambient air. To ensure the objectivity and the impartiality of the results, we chose the PSCs with and without β -CD randomly for the aging measurement, rather than the champion devices exhibited in Fig. 4a. The V_{max} for the maximum power output point measurement of these PSCs was 0.95 V, as shown in Fig. S9.[†] Simultaneously, a Xe lamp without any filter was also employed to provide a continuous illumination on all the PSCs. Even after a continuous illumination for 2000 s, the PSCs with β -CD demonstrated better stability compared to the PSCs without β -CD, as shown in Fig. 4c. The efficiency of PSCs with β -CD maintained 85% of the initial performance, but the efficiency of the PSCs without β -CD has been almost completely degraded. Moreover, the long-term stability of the PSCs without and with β -CD has also been detected. Specifically, we measured the PSCs without encapsulation every 10 hours for 500 hours under AM 1.5G illumination. These PSCs were still kept under continuous illumination with 80% humidity during the measurement intervals. According to Fig. 4d, the long-term stability of the PSCs with β -CD is superior to the PSCs without β -CD. In the first 300 hours, the PCE of PSC with β -CD changed from 20.01% to 18.57%, maintaining 90% of the initial performance. On the contrary, the long-term per-

formance of the PSC without β -CD demonstrated a serious degradation from 17.08% to 0.11% in a shorter period of time. With the increase in the irradiation time to 500 hours, the PCE of the PSC with β -CD reduced slowly to 17.11%, while that of the PSC without β -CD degraded completely. The slow degradation of the PSC with β -CD may be related to the changes in the interlayers between the perovskite and the other functional layers in PSCs.⁴⁵ These indicate that the supramolecular β -CD is beneficial for enhancing the long-term stability of PSCs in humid air conditions.

Conclusion

In summary, the supramolecular macrocycle β -cyclodextrin (β -CD) has been introduced into the perovskite films as an additive to enhance the optoelectronic performance and to improve the stability of PSCs in ambient conditions. These macrocyclic β -CD can improve both the humidity stability and the illumination stability of the perovskite films and devices through the supramolecular interaction between β -CD and the perovskite. In addition, such β -CD materials successfully improve the crystalline properties of perovskite materials and thus, protect the perovskite films underneath from moisture-caused damages. By employing the β -CD molecules, we have achieved the best efficiency of 20.09% with a long-term stability of 500 h for PSCs. This study provides a facile approach to achieve high photovoltaic performance and long-term stability of PSCs by utilizing a macrocyclic molecule as the stability-enhancing additive in the perovskite films, which opens up a new path for introducing organic molecules into PSCs to improve the performance and the stability of the devices.

Experimental section

Device fabrication

In a typical process, ITO glasses ($10 \Omega \text{ sq}^{-1}$) were ultrasonically cleaned three times with deionized water, acetone and isopropyl alcohol for 20 min, respectively. These cleaned and dried substrates were treated by UV ozone for 15 min before using. To prepare the SnO_2 films, the SnO_2 colloid precursor (Alfa) was diluted with deionized water with a volume ratio of 1 : 5 for the SnO_2 precursor solution.⁴⁶ Then, 30 μL of SnO_2 precursor was spin-coated onto the treated ITO glasses at 3000 rpm for 30 s, followed by heating at 150 $^\circ\text{C}$ for 30 min in ambient air. After cooling down to room temperature, these prepared SnO_2 films were treated with UV ozone for 15 min again, before being transferred into a N_2 -filled glove box. To fabricate the perovskite films, the perovskite precursor solution had been prepared as follows: 159 mg of methylammonium iodide (MAI, Xi'an Polymer Light Technology Corp.) and 473 mg of lead iodide (PbI_2 , Alfa) were mixed in 800 μL of *N,N*-dimethylformamide (DMF) and 200 μL of dimethyl sulfoxide (DMSO) (Acros Organics, Extra dry). For comparison, various weights of β -cyclodextrin (β -CD) were dissolved into the above-mentioned

perovskite precursor, and then, the β -CD/perovskite solution (1–20 mg mL^{-1}) was stirred for 2 hours. The perovskite films were fabricated directly on the SnO_2 substrate by spin coating the perovskite precursors with various concentrations of β -CD at 4000 rpm for 30 s. During spin coating, 0.5 mL of chlorobenzene was poured on the surface of the films at 15 s before the end. The prepared films were transferred on to a hot plate to heat at 130 $^\circ\text{C}$ for 15 min, and the heated films converted from light yellow to brownish red. After that, the spiro-OMeTAD solution, which contained 80 mg of the spiro-OMeTAD powder, 28.5 μL of tertbutylpyridine and 17.5 μL of lithiumbis-(trifluoromethanesulfonyl) imide/acetonitrile solution in 1 mL chlorobenzene, was spin coated on the perovskite films at 4000 rpm for 30 s to fabricate the HTM layer. Finally, 80 nm Au was evaporated on the films as the electrode.

Characterization

To investigate the optoelectronic characterizations of the as-prepared films and devices, current–voltage curves of the PSCs were recorded using a source meter (Keithley 2400) under AM 1.5G irradiation with a power density of 100 mW cm^{-2} from a solar simulator (XES-301S + EL-100) by forward (–0.1 V to 1.2 V) or reverse (1.2 V to –0.1 V) scans. The step voltage was fixed at 12 mV and the delay time was set at 10 ms. The chemical compositions of the films were analyzed by X-ray diffraction (XRD) (Bruker D8 Advance X-ray diffractometer, Cu-K α radiation $\lambda = 0.15406 \text{ nm}$). The morphologies of the perovskite films were investigated by scanning electron microscopy (SEM) (FEI SIRION 200). An Edinburg PLS 980 was employed for measuring the static PL spectra of the perovskite films. The external quantum efficiency (EQE) was measured using a QE-R system (Enli Tech.).

Conflicts of interest

There are no conflicts to declare.

Acknowledgements

This study is supported partially by National Natural Science Foundation of China (Grant no. 51772096), Beijing Natural Science Foundation (L172036), Joint Funds of the Equipment Pre-Research and Ministry of Education (6141A020225), Par-Eu Scholars Program, Science and Technology Beijing 100 Leading Talent Training Project, Beijing Municipal Science and Technology Project (Z161100002616039), the Fundamental Research Funds for the Central Universities (2016JQ01, 2017ZZD02) and the NCEPU “Double First-Class” Graduate Talent Cultivation Program.

References

- 1 A. Kojima, K. Teshima, Y. Shirai and T. Miyasaka, *J. Am. Chem. Soc.*, 2009, **131**, 6050.

- 2 W. Yang, J. Noh, N. J. Jeon, Y. C. Kim, S. Ryu, J. Seo and S. H. Im, *Science*, 2015, **348**, 1234.
- 3 Q. Dong, Y. Fang, Y. Shao, P. Mulligan, J. Qiu, L. Cao and J. Huang, *Science*, 2015, **347**, 967.
- 4 M. Saliba, T. Matsui, K. Domanski, J. Y. Seo, A. Ummadisingu, S. M. Zakeeruddin, J. P. Correa-Baena, W. Tress, A. Abate, A. Hagfeldt and M. Graetzel, *Science*, 2016, **354**, 206.
- 5 W. S. Yang, B. W. Park, E. H. Jung, N. J. Jeon, Y. C. Kim, D. U. Lee, S. S. Shin, J. Seo, E. K. Kim, J. H. Noh and S. Seok, *Science*, 2017, **356**, 1376.
- 6 H. Tsai, R. Asadpour, J. C. Blancon, C. C. Stoumpos, O. Durand, J. W. Strzalka, B. Chen, R. Verduzco, P. M. Ajayan, S. Tretiak, J. Even, M. A. Alam, M. G. Kanatzidis, W. Nie and A. D. Mohite, *Science*, 2018, **360**, 67.
- 7 J. H. Im, C. R. Lee, J. W. Lee, S. W. Park and N. G. Park, *Nanoscale*, 2011, **3**, 4088.
- 8 H. S. Kim, C. R. Lee, J. H. Im, K. B. Lee, T. Moehl, A. Marchioro, S. J. Moon, R. Humphry-Baker, J. H. Yum, J. E. Moser, M. Grätzel and N. G. Park, *Sci. Rep.*, 2012, **2**, 591.
- 9 W. S. Yang, J. H. Noh, N. J. Jeon, Y. C. Kim, S. Ryu, J. Seo and S. Seok, *Science*, 2015, **348**, 1234.
- 10 H. Tsai, W. Nie, J. C. Blancon, C. C. Stoumpos, R. Asadpour, B. Harutyunyan, A. J. Neukirch, R. Verduzco, J. J. Crochet, S. Tretiak, L. Pedesseau, J. Even, M. A. Alam, G. Gupta, J. Lou, P. M. Ajayan, M. J. Bedzyk, M. G. Kanatzidis and A. D. Mohite, *Nature*, 2016, **536**, 312.
- 11 X. Li, D. Bi, C. Yi, J. D. Décoppet, J. Luo, S. M. Zakeeruddin, A. Hagfeldt and M. Graetzel, *Science*, 2016, **353**, 58.
- 12 W. S. Yang, B. W. Park, E. H. Jung, N. J. Jeon, Y. C. Kim, D. U. Lee, S. S. Shin, J. Seo, E. K. Kim, J. H. Noh and S. Seok, *Science*, 2017, **356**, 1376.
- 13 NREL Efficiency Chart, http://www.nrel.gov/pv/assets/images/efficiency_chart.jpg.
- 14 G. Niu, W. Li, F. Meng, L. Wang, H. Dong and Y. Qiu, *J. Mater. Chem. A*, 2014, **2**, 705.
- 15 Z. Zhu, V. G. Hadjiev, Y. Rong, R. Guo, B. Cao, Z. Tang, F. Qin, Y. Li, Y. Wang, F. Hao, S. Venkatesan, W. Li, S. Baldelli, A. M. Guloy, H. Fang, Y. Hu, Y. Yao, Z. Wang and J. Bao, *Chem. Mater.*, 2016, **28**, 7385.
- 16 G. E. Eperon, S. N. Habisreutinger, T. Leijtens, B. J. Bruijnaers, J. J. van Franeker, D. W. deQuilettes, S. Pathak, R. J. Sutton, G. Grancini, D. S. Ginger, R. A. J. Janssen, A. Petrozza and H. J. Snaith, *ACS Nano*, 2015, **9**, 9380.
- 17 Q. Tai, P. You, H. Sang, Z. Liu, C. Hu, H. L. W. Chan and F. Yan, *Nat. Commun.*, 2016, **7**, 11105.
- 18 Y. Bai, Q. Dong, Y. Shao, Y. Deng, Q. Wang, L. Shen, D. Wang, W. Wei and J. Huang, *Nat. Commun.*, 2016, **7**, 12806.
- 19 X. Zheng, B. Chen, J. Dai, Y. Fang, Y. Bai, Y. Lin, H. Wei, X. C. Zeng and J. Huang, *Nat. Energy*, 2017, **2**, 17102.
- 20 N. Arora, M. I. Dar, A. Hinderhofer, N. Pellet, F. Schreiber, S. M. Zakeeruddin and M. Graetzel, *Science*, 2017, **358**, 768.
- 21 Y. Zhao, J. Wei, H. Li, Y. Yan, W. Zhou, D. Yu and Q. Zhao, *Nat. Commun.*, 2016, **7**, 10228.
- 22 X. Li, M. I. Dar, C. Yi, J. Luo, M. Tschumi, S. M. Zakeeruddin, M. K. Nazeeruddin, H. Han and M. Graetzel, *Nat. Chem.*, 2015, **7**, 703.
- 23 B. Li, C. Fei, K. Zheng, X. Qu, T. Pullerits, G. Cao and J. Tian, *J. Mater. Chem. A*, 2016, **4**, 17018.
- 24 A. Giuri, S. Masi, S. Colella, A. Listorti, A. Rizzo, A. Liscio, E. Treossi, V. Palermo, G. Gigli, C. Mele and C. E. Corcione, *Nanotechnology*, 2017, **28**, 174001.
- 25 S. Masi, F. Aiello, A. Listorti, F. Balzano, D. Altamura, C. Giannini, R. Caliandro, G. U. Barretta, A. Rizzo and S. Colella, *Chem. Sci.*, 2018, **9**, 3200.
- 26 D. Wei, F. Ma, R. Wang, S. Dou, P. Cui, H. Huang, J. Ji, E. Jia, X. Jia, S. Sajid, A. M. Elseman, L. Chu, Y. Li, B. Jiang, J. Qiao, Y. Yuan and M. Li, *Adv. Mater.*, 2018, **30**, 1707583.
- 27 D. Wei, T. Wang, J. Ji, M. Li, P. Cui, Y. Li, G. Li, J. M. Mbengue and D. Song, *J. Mater. Chem. A*, 2016, **4**, 1991.
- 28 D. Song, J. Ji, Y. Li, G. Li, M. Li, T. Wang, D. Wei, P. Cui, Y. He and J. M. Mbengue, *Appl. Phys. Lett.*, 2016, **108**, 093901.
- 29 D. Song, D. Wei, P. Cui, M. Li, Z. Duan, T. Wang, J. Ji, Y. Li, J. M. Mbengue, Y. Li, Y. He, M. Trevor and N. G. Park, *J. Mater. Chem. A*, 2016, **4**, 6091.
- 30 D. Wei, J. Ji, D. Song, M. Li, P. Cui, Y. Li, J. M. Mbengue, W. Zhou, Z. Ning and N. G. Park, *J. Mater. Chem. A*, 2017, **5**, 1406.
- 31 D. Song, P. Cui, T. Wang, D. Wei, M. Li, F. Cao, X. Yue, P. Fu, Y. Li, Y. He, B. Jiang and M. Trevor, *J. Phys. Chem. C*, 2015, **119**, 22812.
- 32 P. Cui, D. Wei, J. Ji, D. Song, Y. Li, X. Liu, J. Huang, T. Wang, J. You and M. Li, *Sol. RRL*, 2017, 1600027.
- 33 Z. Zhang, D. Wei, B. Xie, X. Yue, M. Li, D. Song and Y. Li, *Sol. Energy*, 2015, **122**, 97.
- 34 Z. Zhang, M. Li, W. Liu, X. Yue, P. Cui and D. Wei, *Sol. Energy Mater. Sol. Cells*, 2017, **163**, 250.
- 35 W. Ke, C. Xiao, C. Wang, B. Saparov, H. Duan, D. Zhao, Z. Xiao, P. Schulz, S. P. Harvey, W. Liao, W. Meng, Y. Yu, A. J. Cimaroli, C. Jiang, K. Zhu, M. Al-Jassim, G. Fang, D. B. Mitzi and Y. Yan, *Adv. Mater.*, 2016, **28**, 5214.
- 36 X. Zhu, D. Yang, R. Yang, B. Yang, Z. Yang, X. Ren, J. Zhang, J. Niu, J. Feng and S. Liu, *Nanoscale*, 2017, **9**, 12316.
- 37 V. Innocenzo, A. R. S. Kandada, M. D. Bastiani, M. Gandini and A. Petrozza, *J. Am. Chem. Soc.*, 2014, **136**, 17730.
- 38 T. Bu, X. Liu, Y. Zhou, J. Yi, X. Huang, L. Luo, J. Xiao, Z. Ku, Y. Peng, F. Huang, Y. Cheng and J. Zhong, *Energy Environ. Sci.*, 2017, **10**, 2509.
- 39 D. Son, J. Lee, Y. Choi, I. Jang, S. Lee, P. J. Yoo, H. Shin, N. Ahn, M. Choi, D. Kim and N. G. Park, *Nat. Energy*, 2016, **1**, 16081.
- 40 Y. Zhao, H. Tan, H. Yuan, Z. Yang, J. Z. Fan, J. Kim, O. Voznyy, X. Gong, L. N. Quan, C. S. Tan, J. Hofkens,

- D. Yu, Q. Zhao and E. H. Sargent, *Nat. Commun.*, 2018, **9**, 1607.
- 41 Q. Chen, H. Zhou, T. Song, S. Luo, Z. Hong, H. Duan, L. Dou, Y. Liu and Y. Yang, *Nano Lett.*, 2014, **14**, 4158.
- 42 C. Roldan-Carmona, P. Gratia, I. Zimmermann, G. Grancini, P. Gao, M. Gratzel and M. K. Nazeeruddin, *Energy Environ. Sci.*, 2015, **8**, 3550.
- 43 M. I. Saidaminov, J. Kim, A. Jain, R. Quintero-Bermudez, H. Tan, G. Long, F. Tan, A. Johnston, Y. Zhao, O. Voznyy and E. H. Sargent, *Nat. Energy*, 2018, **3**, 648.
- 44 S. Li, C. Chang, Y. Wang, C. Lin, D. Wang, J. Lin, C. C. Chen, H. Sheu, H. Chia, W. Wu, U. Jeng, C. Liang, R. Sankar, F. Chou and C. W. Chen, *Energy Environ. Sci.*, 2016, **9**, 1282.
- 45 K. Domanski, J. Correa-Baena, N. Mine, M. K. Nazeeruddin, A. Abate, M. Saliba, W. Tress, A. Hagfeldt and M. Gratzel, *ACS Nano*, 2016, **6**, 6306.
- 46 Q. Jiang, L. Zhang, H. Wang, X. Yang, J. Meng, H. Liu, Z. Yin, J. Wu, X. Zhang and J. You, *Nat. Energy*, 2017, **2**, 16177.